

Distribution Agreement

In presenting this thesis as a partial fulfillment of the requirements for a degree from Emory University, I hereby grant to Emory University and its agents the non-exclusive license to archive, make accessible, and display my thesis in whole or in part in all forms of media, now or hereafter now, including display on the World Wide Web. I understand that I may select some access restrictions as part of the online submission of this thesis. I retain all ownership rights to the copyright of the thesis. I also retain the right to use in future works (such as articles or books) all or part of this thesis.

Sindhu Potlapalli

April 14, 2020

BMI-1 Inhibition and Hippo Signaling in Alveolar Rhabdomyosarcoma

by

Sindhu Potlapalli

Robert Schnepf
Adviser

Department of Biology

Robert Schnepf
Adviser

Anita Corbett
Committee Member

Jennifer Heemstra
Committee Member

2020

BMI-1 Inhibition and Hippo Signaling in Alveolar Rhabdomyosarcoma

By

Sindhu Potlapalli

Robert Schnepf
Adviser

An abstract of
a thesis submitted to the Faculty of Emory College of Arts and Sciences
of Emory University in partial fulfillment
of the requirements of the degree of
Bachelor of Science with Honors

Department of Biology

2020

Abstract
BMI-1 Inhibition and Hippo Signaling in Alveolar Rhabdomyosarcoma
By Sindhu Potlapalli

Alveolar rhabdomyosarcoma (ARMS) is a prevalent pediatric soft-tissue sarcoma with poor prognosis in high-risk patients. Recent research shows that BMI-1, an epigenetic histone repressor and stem cell factor, expresses a significant oncogenic effect within many cancers. Interestingly, one of these effects is on the Hippo protein pathway. Utilizing western blot analysis, Annexin V/PI staining, and BrdU/7-AAD staining on siRNA-induced and PTC-028 drug-induced BMI-1 downregulated ARMS cells, we examined the effects of BMI-1 inhibition on Hippo pathway proteins and on cellular apoptosis and the cell cycle. We found that BMI-1 inhibition rescues the Hippo pathway at LATS1/2 in the ARMS Rh30 cell line, upregulating phosphorylation at core Hippo pathway proteins LATS1/2 and possibly YAP. Furthermore, in Rh28, PTC-028 mediated BMI-1 inhibition may turn on the Hippo pathway at MST1. BMI-1 inhibition by drug and siRNA has also shown an increase in apoptosis and decrease in proliferation in tumorigenic ARMS cells. Hence, study of cancer pathway effects of BMI-1 has validated its potential as a powerful target of PTC-028 drug therapy, providing a clinical method to restore cell cycle arrest and repair and apoptotic processes in pediatric rhabdomyosarcomas.

BMI-1 Inhibition and Hippo Signaling in Alveolar Rhabdomyosarcoma

By

Sindhu Potlapalli

Robert Schnepf
Adviser

A thesis submitted to the Faculty of Emory College of Arts and Sciences
of Emory University in partial fulfillment
of the requirements of the degree of
Bachelor of Science with Honors

Department of Biology

2020

Acknowledgements

First, I would like to thank Dr. Robert Schnepf for all his guidance in this project. His lab was my first experience with research in which I was able to develop and guide my own project. As a hopeful for medical school, I had always wanted to research something clinically relevant and I am very grateful for being able to work with Dr. Schnepf on research that could impact medicine.

Moreover, I must thank Cara Shields for being my graduate student mentor. Working closely with her has taught me greatly about the laboratory experience and how to conduct research. She has helped me conduct experiments and even provided some data for my thesis.

*Asterisked data in the thesis are figures provided by Cara.

Also, I would like to thank other members of the lab, past and present; namely, Julie Chen, Adeiye Pilgrim, and Selma Cuya for being there for me and all my questions. I thank everyone for their patience and their help.

Lastly, I'd like to thank my committee members Dr. Anita Corbett and Dr. Jennifer Heemstra for their valuable input. Even if I could not implement all their advice, I appreciate their commitment to seeing me through my thesis.

Table of Contents

- I. Introduction and Literature Review.....1**
 - A. Introduction to Cancer.....1*
 - B. Overview of Rhabdomyosarcoma.....3*
 - C. Novel epigenetic target, BMI-1.....6*
 - D. Overview of the Hippo Pathway.....8*
 - E. BMI-1 Inhibitor, PTC-028.....10*
 - F. Hypotheses and Aims.....11*
- II. Materials and Methods.....12**
- III. Results.....14**
 - A. Knockdown Determination of BMI-1.....14*
 - B. Determining BMI-1 interactions with the Hippo Pathway.....;.....16*
 - C. Determining effects of BMI-1 on overall cell cycle and vitality.....20*
- IV. Discussion.....24**
 - A. siRNA Transfection Validation.....24*
 - B. BMI-1 Inhibition Turns on the Hippo Pathway.....25*
 - C. BMI-1 inhibition increases cellular apoptosis and diminishes progression to S-phase.....28*
- V. Further Research and Conclusions.....31**
- VI. Bibliography.....33**
- VII. Non-Print References.....36**
- Appendix A: Supplementary Figures.....37**

Figures

I.	Figure 1. Therapeutics that target the hallmarks of cancer, <i>Hanahan and Weinberg, 2011</i>	1
II.	Figure 2. Occurrence of most common pediatric cancer subsets based on data provided by <i>ACS Cancer Facts and Figures, 2019</i>	3
III.	Figure 3. Occurrence of ARMS subtypes based on data provided by (Barr, 2009).....	4
IV.	Figure 4. Ubiquitination of histone H2A by BMI-1 and the PRC1 complex.....	6
V.	Figure 5. BMI-1 associated cancer pathways.....	7
VI.	Figure 6. Overview of the Hippo Pathway.....	8
VII.	Figure 7. Molecular structure of PTC-028 <i>from Selleckchem</i>	10
VIII.	Figure 8. Knockdown validation of BMI-1 in the Rh30 cell line.....	14
IX.	Figure 9. Knockdown validation of BMI-1 in the Rh28 cell line.....	15
X.	Figure 10. Hippo pathway proteins in siRNA inhibition of BMI-1 in Rh30.....	16
XI.	Figure 11. Hippo pathway protein in PTC-028 inhibition of BMI-1 in Rh28 and Rh30.....	18
XII.	Figure 12. BMI-1 inhibition by siRNA effects on potential downstream regulators of the Hippo cascade.....	19
XIII.	Figure 13. BMI-1 inhibition by siRNA effects on apoptosis in Rh30.....	20
XIV.	Figure 14. BMI-1 inhibition by PTC-028 effects on apoptosis of Rh28, Rh30, and Rh41...21	
XV.	Figure 15. Cell cycle effects of BMI-1 inhibition by PTC-028 in Rh30.....	22
XVI.	Figure S1. Magnification of select protein expression differences in Rh30 between siCTL and siBMI-1 treatments through western blot protein quantification.....	37
XVII.	Figure S2. Top 10 genes in NanoString analysis that show differential expression from PTC-028 vs baseline of control in Rh28 and Rh30.....	37
XVIII.	Figure S3. Failed siBMI-1 knockdown validation in Rh30 siRNA treated cells.....	38
XIX.	Figure S4. BMI-1 inhibition by PTC-028 effects on apoptosis shown by Annexin V/PI staining and western blot of cleaved PARP.....	38

I. Introduction and Literature Review

A. Introduction to Cancer

Since the late twentieth century, cancer has become an increasingly prevalent leading cause of death around the world. It is the result of uncontrolled cell growth, where cells become independent of controls such as intracellular and intercellular signals. In normal cells, these intricate signaling pathways utilize feedback mechanisms to keep the body functioning smoothly. For the transformation from a normal cell to an aberrant cancer cell, multiple molecular changes must first occur. These changes often occur in genes that control various hallmarks of cancer, including evading growth suppressors, inducing angiogenesis, resisting cell death, etc. (Figure 1). Most cancer therapies are focused on targeting these few common traits cancers share, hence their designation as hallmarks. However, the fallacy in this approach is that cancer is a category of diseases unique for its vast individual diversity.

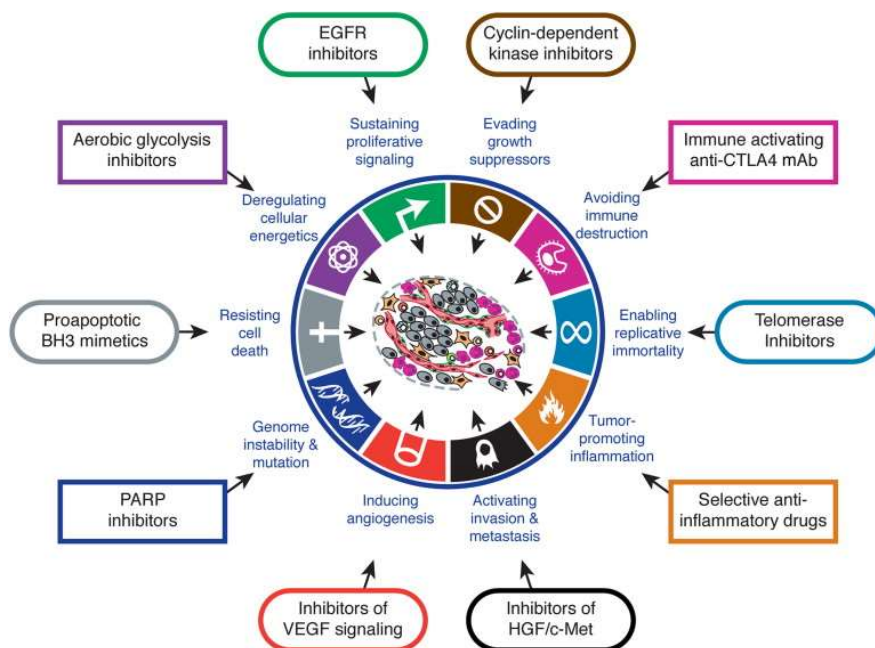


Figure 1. Therapeutics that target the hallmarks of cancer, *Hanahan and Weinberg, 2011*

Cancer is considered a disease of aging. Cancer prevalence and incidence rates climb up in a logarithmic manner per each age interval, with the 75+ age interval reaching a morbidity rate near 2300 cases per 100,000 people while the 1-34 age interval all have age-specific rates less than 100 cases per 100,000 people (U.S. Cancer Statistics Working Group, 2019). The molecular basis of cancer occurrence explains this logistic increase of cancer incidence by age. Cancer is ultimately a genetic disease, wherein mutations at key genes can set the path forward for subsequent mutation accumulation. And mutation accumulation is an inherent process of time, where random mutations during DNA synthesis occur as normal cellular regeneration processes continue over a lifetime. This accumulation of mutations contributes to the tumor heterogeneity that necessitates multiple therapeutic approaches to optimize treatment.

Overall cancer estimates in 2019 show that of the 1,762,450 new cases and 606,880 deaths, only 11,060 new cases and 1,190 deaths are due to pediatric cancers (American Cancer Society, 2019). Even though pediatric cancers are statistically rarer, it is the leading cause of death by disease in children aged 0-14. 1 in 500 children will be diagnosed with cancer by age 15 (American Cancer Society, 2019). Thus, pediatric cancer is a significant area of clinical research. However, because of the rarity of patients, pediatric cancer is also a challenging field of research.

B. Overview of Rhabdomyosarcoma

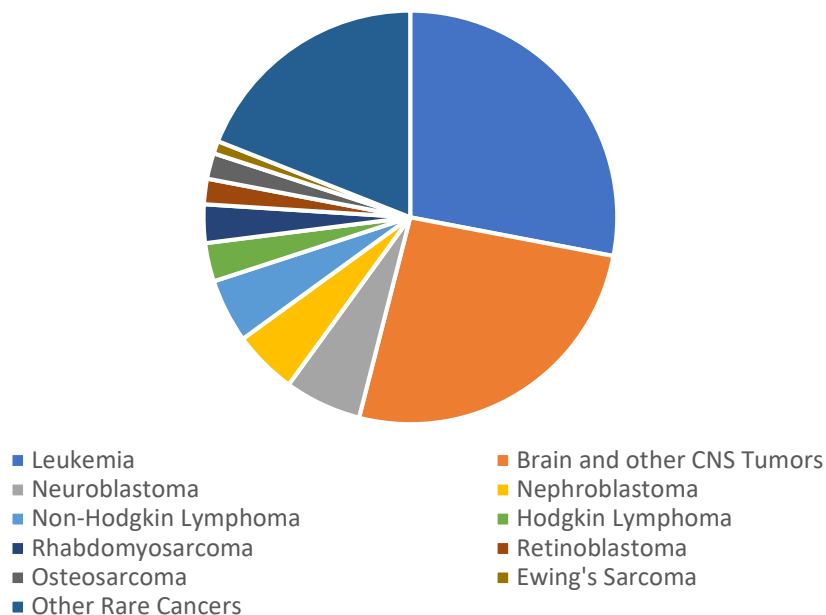


Figure 2. Occurrence of most common pediatric cancer subsets based on data provided by ACS *Cancer Facts and Figures, 2019*

While the most common pediatric cancers are leukemia (occurring in 28% of cases) and CNS tumors (26% of cases), sarcomas also comprise a small but significant portion of cases (Figure 2). Rhabdomyosarcoma and Ewing's Sarcoma, specifically, are soft-tissue sarcomas (STS), rare tumors that comprise 1% of adult malignancies but make up 12% of pediatric cancers (Lim et. al., 2015). STS are dangerous cancers that originate from mesenchymal cells, arising in the connective tissue of bones, muscles, tendons, and other limb tissues.

Rhabdomyosarcoma is a highly aggressive and malignant subset of the already generally aggressive soft-tissue sarcoma. While the exact origins of rms continue to be investigated, it likely originates from skeletal muscle tissues that have failed to fully differentiate. It has a very low 5-year survival compared to other common childhood cancer, with a survival of 70%

(American Cancer Society, 2018). There are three main types of rhabdomyosarcoma: alveolar (ARMS), embryonal (ERMS), and pleomorphic (PRMS) rhabdomyosarcoma. ARMS is the most not true aggressive form of rhabdomyosarcoma, with primary tumors found mostly in the extremities and the trunk. High-risk ARMS patients only have a 20-30% 5-year survival (American Cancer Society, 2018), while the survival rate for ERMS is much higher, underscoring the importance of identifying novel potential therapeutic targets for ARMS.

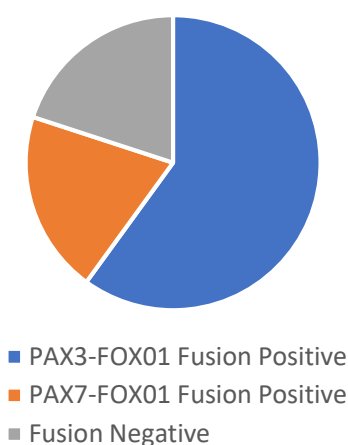


Figure 3. Occurrence of ARMS subtypes based on data provided by (Barr, 2009)

Alveolar rhabdomyosarcoma can be further categorized by genotype. 80% of ARMS is fusion-positive (Figure 3), meaning that it be characterized by a fusion protein created by either a 2;13 or 1;13 chromosomal translocation. The 2;13 translocation occurs in 75% of fusion-positive ARMS cases, forming the PAX3-FOX01 oncogene. The fusion protein expressed from this oncogene is a novel transcription factor that is currently undruggable.

The current treatments for ARMS include surgery, radiation, and chemotherapy with significant side effects. These cancer therapies are unsatisfactory because children may respond differently to drugs that control symptoms in adults. Moreover, cancer treatments have different and dangerous effects on developing bodies that are more negligible in adult bodies.

Children may receive more intense treatments that cause greater late effects. Survivors of any kind of cancer can develop health problems, i.e. late effects, years after harsh cancer treatments. Late effects are of particular concern for childhood cancer survivors because these treatments on developing bodies can cause profound, lasting physical and emotion effects. Unfortunately, there are no current targeted therapies for ARMS that may augment or potentially one day replace these current treatments.

Thus, the need for a novel target therapy becomes evident. Recently, epigenetic targets have been demonstrating increasing clinical relevance. Disruptions by a relatively small subset of mutated or aberrantly expressed epigenetic proteins are strong contributors to pediatric solid tumor pathogenesis (Lawlor and Thiele, 2012). Furthermore, therapies against these epigenetic targets have shown to combine well with standard of care chemotherapies. One such target is the Polycomb Group (PcG) protein BMI-1 (B lymphoma Mo-MLV insertion dregion 1 homolog).

C. *Novel epigenetic target, BMI-1*

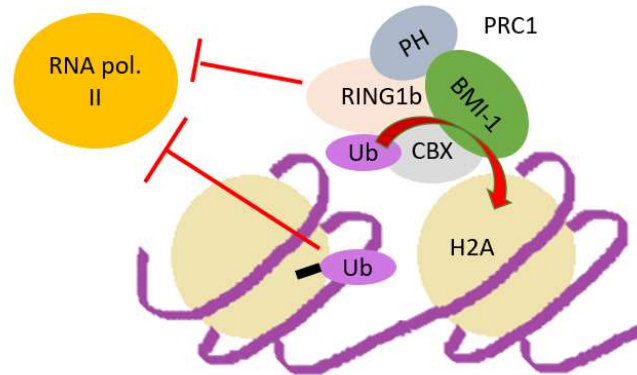


Figure 4. Ubiquitination of histone H2A by BMI-1 and the PRC1 complex

Overexpression of PcGs are associated with tumor suppressor inhibition, proliferation, cell death, senescence resistance, and invasion (Wang et. al., 2015). There are two main PcG complexes, PRC1 (polycomb repressor complex 1) and PRC2, both of which contribute to chromatin compaction by ubiquitinating histones H2AK119 and H3K27 respectively (Chittock et. al., 2017). BMI-1 is an epigenetic gene silencer that participates in ubiquitination of histone H2A through the PRC1 complex to regulate chromatin structure (Figure 4). BMI-1 is also a stem cell factor that controls homeotic developmental genes in its normal function and is crucial for regulation of genomic programming and differentiation; when deregulated, it contributes to the proliferation and self-renewal of tumor cells (Schwartz and Pirrota, 2008).

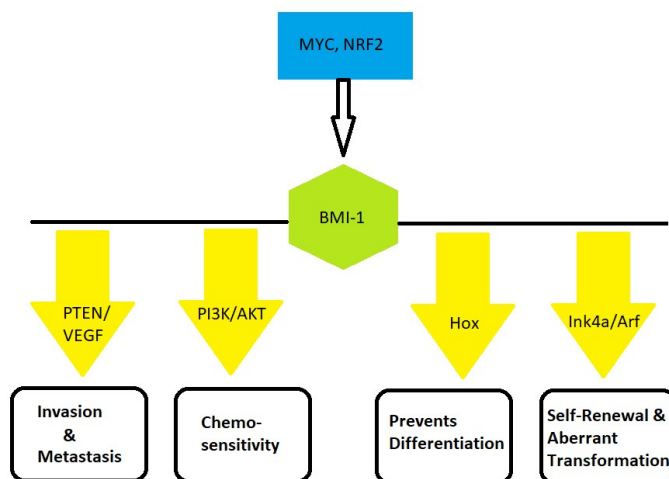


Figure 5. BMI-1 associated cancer pathways

BMI-1 is positively correlated with MYC, a protein family associated with development and tumorigenesis, for MYC directly transcriptionally activates BMI-1 in neuroblastoma tumorigenesis (Huang et al., 2011). Further studies have shown that BMI-1 is involved in multiple cancer pathways, including EMT, angiogenesis, cancer stem cell renewal, and cell cycle dysregulation (Figure 5, Richly et al., 2011). Thus, BMI-1's presence in the various cancer pathways increases its potential as a target for an effective therapy in alveolar rhabdomyosarcoma.

D. Overview of the Hippo Pathway

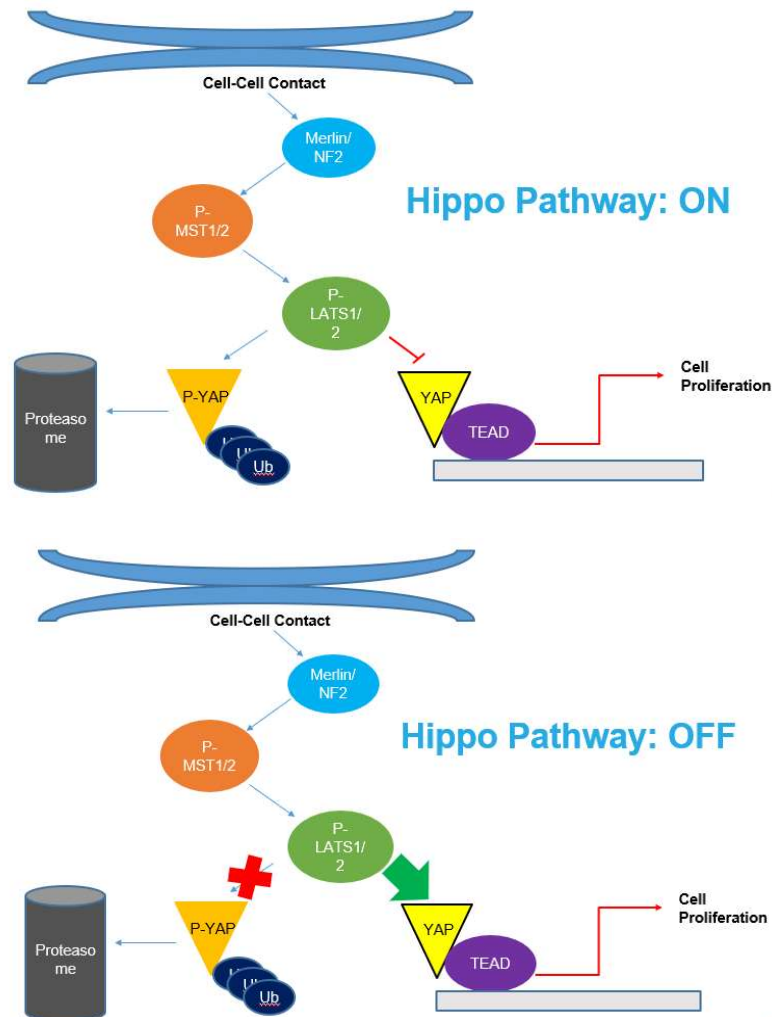


Figure 6. Overview of the Hippo Pathway

Interestingly, BMI-1 has recently shown significant interactions with the tumor-suppressing Hippo pathway in Ewing's sarcoma (Hsu and Lawlor, 2010). The Hippo pathway is a highly conserved, major regulatory pathway for organ growth and organ cell proliferation that controls contact inhibition of tissues.

The Hippo pathway is an intrinsic mechanism of the body that influences the regulation of organ size. It was first discovered in *Drosophila* and was later shown to be conserved among vertebrates (Halder and Johnson, 2011). The core proteins of the Hippo kinase cassette are MST1/2 (human orthologue to *Hpo* in *Drosophila*), LATS1/2 (*Wts* in *Drosophila*), and YAP (*Yki* in *Drosophila*) (Staley and Irvine, 2012). Merlin, also known as Neurofibromin 2 (NF2), is a cytoskeletal scaffolding protein that acts as a tumor suppressor and is an upstream regulator of the Hippo pathway. Mutations in this gene lead to nervous system tumor development, most commonly schwannomas (Scoles et. al, 2006). Knockout of *Hpo* in *Drosophila*, and its orthologue MST1/2 in mice, shows unencumbered organ growth (Halder and Johnson, 2011). In *Drosophila*, knockout of *Wts* (LATS1/2) resulted in robust overgrowth in multiple tissues (Justice et. al., 1995), while knockout of LATS1/2 in mice led to the development of ovarian tumors and soft-tissue sarcomas (St. John et. al., 1999).

Figure 6 shows that when two cells contact each other, Merlin, among other upstream cytoskeletal proteins, is signaled to turn on the Hippo pathway. Merlin initiates a signaling pathway to phosphorylate the MST1/2 kinase in the cytoplasm. MST1/2 consequently phosphorylates LATS1/2. The activated LATS1/2 phosphorylate YAP. YAP phosphorylation targets it for polyubiquitination to send YAP for proteasomal degradation. If YAP is not phosphorylated, when the Hippo pathway is turned off, it progresses to the nucleus with its co-activator, TAZ (not pictured), to activate the TEAD transcription factor family. YAP and TEADs both promote cell proliferation and aberrant transformation of normal cells to cancer cells.

In Ewing's sarcoma, BMI-1 is positively correlated with YAP levels, such that BMI-1 knockdown demonstrated progressive downregulation of YAP as well as decrease in cell density

(Hsu and Lawlor, 2010). Thus, BMI-1 may have a powerful role in inhibiting the Hippo pathway to upregulate YAP protein during cell proliferation.

E. BMI-1 inhibitor, PTC-028

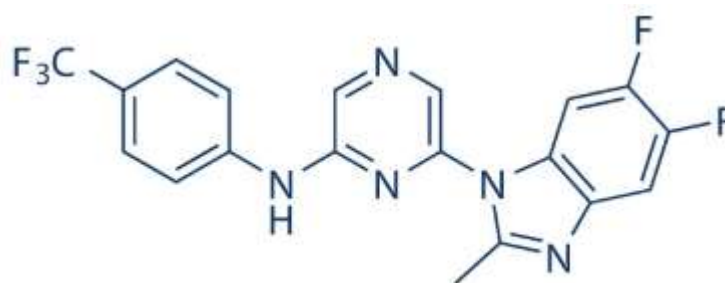


Figure 7. Molecular structure of PTC-028 from Selleckchem

To target BMI-1, there are small molecule inhibitors that have been tested in other cancers, PTC-028. PTC-028 depletes BMI-1 by causing hyperphosphorylation-mediated degradation, which has been shown to induce reduction of cellular ATP and consequent induction of apoptosis-initiating mitochondrial ROS (Dey et. al., 2018). PTC-028 has been highly effective in mice tumor reduction *in vivo*, suggesting that targeting BMI-1 may sensitize many cancers to chemotherapies and reduce tumors (Schwartz and Pirrotta, 2008). Moreover, PcG proteins, such as BMI-1, have shown direct interactions with the Hippo signaling cascade in *Drosophila* (Parrish et. al., 2007). Hence, understanding BMI-1's downstream effects on the Hippo pathway may be promising for translation of PTC-028 to the clinic.

F. Hypotheses and Aims

We hypothesized that BMI-1 inhibition would promote the Hippo cascade through pathway proteins MST1/2, LATS1/2, and YAP. We also hypothesized that BMI-1 inhibition would decrease cell cycle progression and increase apoptosis. Hence, Aim 1 was to establish BMI-1 effects on Hippo pathway expression using siRNA knockdown and inhibition by PTC-028. Our second aim was to elucidate BMI-1 inhibition effects on the cell cycle and apoptosis, through siRNA knockdown and PTC-028 treatment. By doing so, we hoped to understand and gain a therapeutic perspective on BMI-1 as a target so that this research would be translationally relevant and result in novel treatment options for patients with ARMS.

II. Materials and Methods

Cell Culture: Alveolar rhabdomyosarcoma cell lines Rh30 and Rh41 were obtained from the Children's Hospital of Philadelphia (Courtesy of Dr. Margaret Chou), while Rh28 was provided by the Children's Oncology Group. The cell lines were authenticated by the Emory Genomics Core and were tested with the *Mycoplasma* test kit (PromoCell, PK-CA91-10124) every 3-6 months for contamination. Cells were cultured in an incubator at 37 °C with 5% CO₂, with Rh30 having been passaged regularly in DMEM (Corning) and Rh28 and Rh41 in RPMI 1640 (Corning). 10% FBS (Corning) and 1% L-glutamine (Geminin) were added to the DMEM and RPMI 1640 media, with no addition antibiotics or antimycotics.

siRNA Transfection: Rh28 and Rh30 cells were plated at 200,000 cells per well in a 6-well plate. After a 24-hour period, cells were transfected with either 25 nM of ON-TARGET Plus SMARTpool BMI-1 siRNA (Horizon Discovery) or ON-TARGET Plus Non-targeting Control siRNA (Horizon Discovery), employing DharmaFECT1 (Horizon Discovery) as the transfection agent.

Real-Time PCR: The RNeasy Mini Kit (QIAGEN) was utilized to isolate RNA from siRNA-transfected Rh28 and Rh30 cells per manufacturer's instructions, and quantitative Real-Time PCR (qRT-PCR) analysis was performed on *BMI-1* mRNA.

Western Blots: Cell samples were lysed with RIPA buffer (Boston Bioproducts) containing cOmplete protease inhibitor cocktail (Roche) and PMSF (Cell Signaling Technology), then sonicated. Bradford assays (Bio-Rad) determined protein concentrations for standardization of samples. Samples were either run at 15 µg or 50 µg (only for YAP and p-YAP blots) on SDS PAGE Bis-Tris 4-12% gels (Life Technologies). These gels were transferred to nitrocellulose

membranes, which were blocked with 5% Blotting-Grade Blocker (Bio-Rad) in Tris-Buffered Saline with 1% Tween-20 (Cell Signaling Technology). The blots were then incubated overnight with primary anti-Rabbit antibodies (Cell Signaling Technologies) at 1:1000 dilution in 5% BSA (Jackson Laboratory) at 4 °C. Blots were then incubated with IRDye 800CW/680RD anti-Rabbit (Li-COR Biosciences) secondary antibody at 1:50,00 dilution, after which they were scanned with the Li-COR Odyssey. Any quantifications presented were performed with ImageJ and are exhibited as relative adjusted densities (Figure 8C and S1).

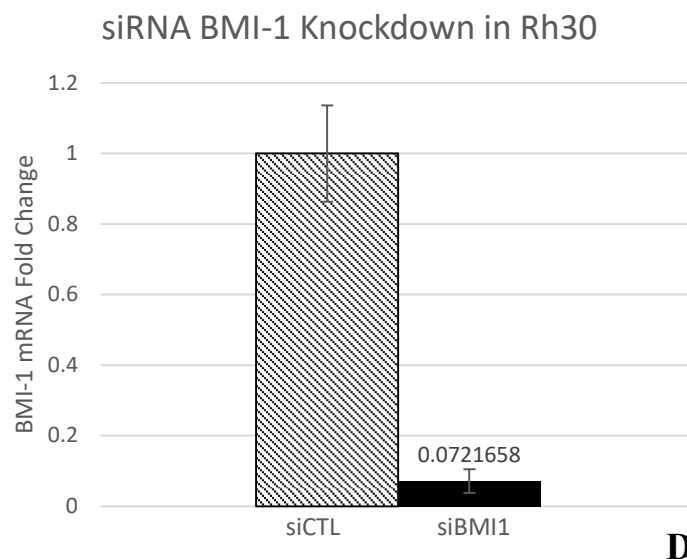
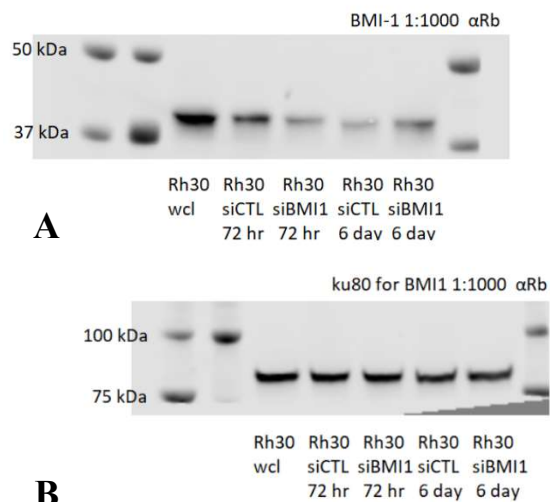
Flow Cytometry: For RNAi based inhibition studies, Rh30 cells were seeded according to siRNA transfection protocol described above. 72 hours post-transfection, cells were harvested and stained with the Annexin V-FITC/PI (BD Biosciences) kit following manufacturer's guidelines. Cell media supernatant containing dead cells was collected and analyzed with live cells.

For drug-based inhibition studies, Rh28, Rh30, and Rh41 cells were seeded at 1 million/10 cm plate. They were treated with PTC-028 after a 24-hour period and harvested 48 hours after that. They were stained with Annexin V-FITC/PI or BrdU-APC/7-AAD (BD Biosciences) kits following manufacturer's guidelines. Again, for the Annexin V/PI staining, dead cells in the supernatant were collected and analyzed with live cells.

All analysis proceeded after samples were run within 1 hour on a Cytoflex 96 well plate loader. 50,000 or 100,000 events were collected per sample and compensation, gating, and analyses were performed in FlowJo.

III. Results

A. Knockdown Determination of BMI-1



BMI-1 Protein Quantification in Rh30

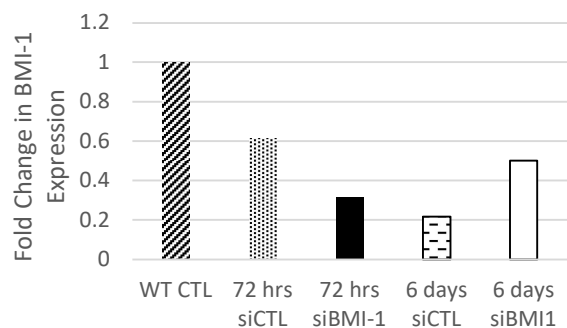


Figure 8. Knockdown validation of BMI-1 in the Rh30 cell line. Western blot analysis and protein quantification of western blot performed on Rh30 lysates 72 hours and 6 days after siRNA transfection (A-C), with antibodies targeting BMI-1 (A) and ku80 as the protein loading control (B). qRT-PCR performed on RNA collected from Rh30 lysates transfected with siRNA for 72 hours (D).

ARMS Rh30 lysates were transfected with either siRNA against the *BMI-1* gene or scrambled siRNA over a 3 or 6-day period. Transfected Rh30 lysates at 72 hours show a 48.4% fold decrease in BMI-1 proteins from lysates transfected with siCTL, and a 68.5% fold decrease

from untreated lysates; however, there is a 56.7% fold increase in lysates treated with siBMI-1 at 6 days compared to those treated with siCTL (Figure 8A and 8C). From this point onwards, only lysates treated with siRNA at 72 hours were analyzed.

Furthermore, BMI-1 mRNA levels show a 92.8% fold decrease in Rh30 samples treated with siBMI-1 for 72 hours compared to those treated with siCTL (Figure 8D). Standard deviation for qRT-PCR siCTL samples are 0.137 and 0.034 for siBMI-1 samples.

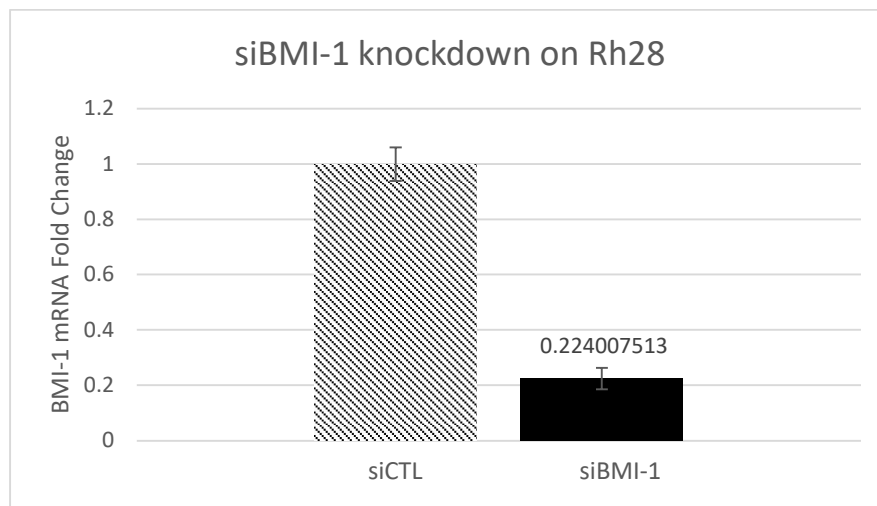


Figure 9. Knockdown validation of BMI-1 in the Rh28 cell line. qRT-PCR performed on RNA collected for Rh28 lysates transfected with siRNA for 72 hours

Cells from the ARMS Rh28 cell line were also transfected with either siRNAs targeting *Bmi1* or scrambled siRNAs for 72 hours, and then lysed. BMI-1 mRNA extracted from these lysates shows a 77.6% fold decrease from control samples (Figure 9). Standard deviation for qRT-PCR siCTL samples are 0.061 and 0.039 for siBMI-1 samples.

B. Determining BMI-1 interactions with the Hippo Pathway

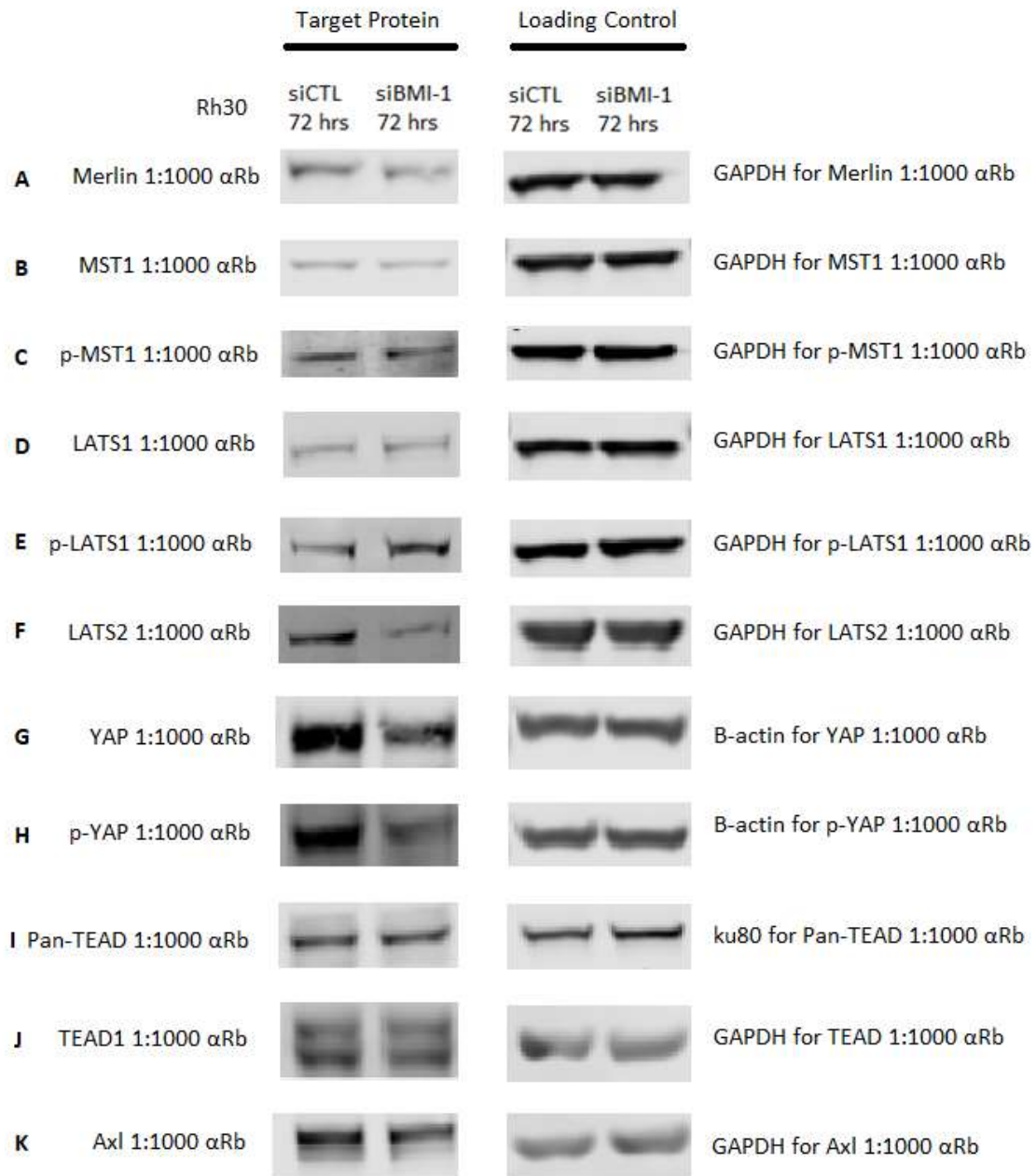


Figure 10. Hippo pathway proteins Merlin (A), MST1 (B-C), LATS1/2 (D-F), YAP (G-H), TEADs (I-J), and Axl (K) in siCTL and siBMI-1 treatments with protein loading controls in Rh30.

In Rh30, the effects of BMI1 on major Hippo pathway proteins Merlin, also known as NF2, MST1, LATS1/2, and YAP were assessed through western blot analysis. Compared to the siCTL treatment in Rh30, Merlin and MST1 protein levels seem to decrease very slightly in the Rh30 siBMI-1 treatment, though this was uncertain (Figures 10A and 10B). Hence, western blots for Merlin and MST1, in which there was uncertainty in differences between protein levels, were quantified and the fold change differences were magnified. These quantifications also suggest a slight fold decrease in the siBMI-1 treatment compared to siCTL, larger for Merlin than for MST1 (Figure S1).

Phosphorylated MST1 shows a slight fold decrease in the siBMI-1 treatment compared to control in Rh30 (Figure 10C). On the other hand, p-LATS1 in the siBMI-1 treatment shows a salient fold increase compared to the LATS1 western blot, which showed no difference between both treatments (Figure 10D and 10E). Moreover, LATS2 shows a substantial fold decrease from the control in the siBMI-1 treatment (Figure 10F).

Both YAP and p-YAP show a clear fold decrease in the siBMI-1 treatment compared to control (Figure 10G and 10H). Moreover, an analysis of just TEAD1 or all TEADs (TEADs 1-4), which are the direct activation targets of YAP, show no considerable difference in protein levels between the siCTL and siBMI-1 treatments in Rh30 (Figure 10I and 10J). Hence, protein expression of the downstream target of YAP-dependent signaling, Axl, was assessed in the Rh30 siBMI-1 treatment, showing a very slight fold decrease (Figure 10K).

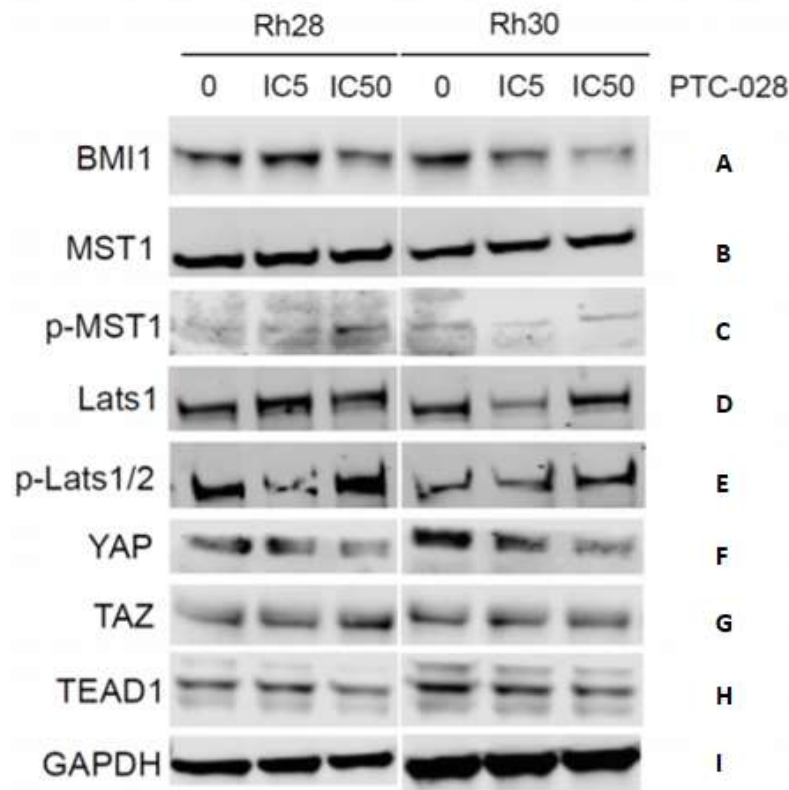


Figure 11. BMI-1 (A) inhibition effects on Hippo pathway proteins MST1 (B-C), LATS1/2 (D-E), YAP (F), TAZ (G), and TEAD1 (H) in PTC-028 treatments with protein loading control GAPDH (I) in Rh28 and Rh30*

PTC-028 shows inhibition of BMI-1 in both Rh28 and Rh30, although to a greater extent in Rh30 (Figure 11A). Therefore, western blot analyses of core Hippo pathway proteins show similar differential expression between increasing PTC-028 drug treatment and siRNA inhibition of BMI-1 in Rh30. p- LATS1/2 increases in expression as the drug is increased in Rh30, and presumably in Rh28 (Figure 11E). YAP clearly decreases in expression as the drug increases in Rh30 and does so at IC50 in Rh28 (Figure 11F).

However, there are a few differences in expression patterns in Rh28 compared to Rh30. While MST1 levels do not change in both Rh28 or Rh30 as drug increases, p-MST1 increases at

IC50 of drug treatment in Rh28 (Figures 11B and 11C). In Rh30, matching the siBMI-1 treatment trend, p-MST1 seems to drop at IC5 and increase at IC50, but never to DMSO-treated levels (Figure 11C). For Rh28, LATS1 increases at IC5 but returns to DMSO-treated levels at IC50, while it decreases at IC5 and returns to DMSO-treated levels at IC50 (Figure 11D). YAP's co-activator TAZ does not change substantially as drug increases in Rh28 or Rh30 (Figure 11G). TEAD1 did seem to decrease with increasing drug treatment in both cell lines (Figure 11H).

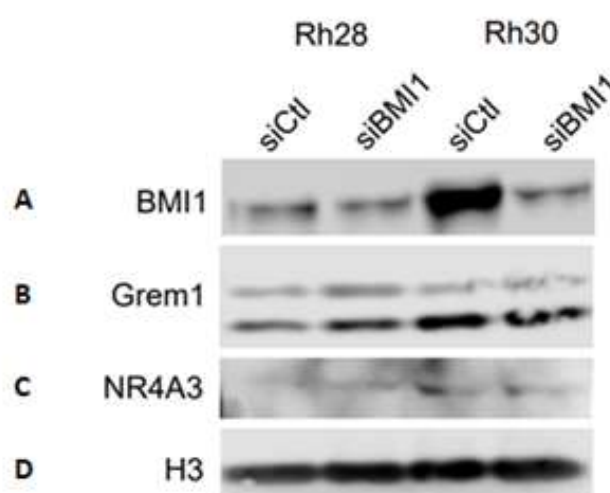


Figure 12. BMI-1 (A) inhibition effects on (B) GREM1, and (C) NR4A3 with (D) H3 protein loading control in Rh28 and Rh30, comparing siCTL to siBMI-1 treatments*

To identify additional BMI-1 influenced genes, we utilized NanoString of Rh28 and Rh30 cells, performing the analysis in both control and PTC-028 cells. The NanoString analysis identified Grem1 and NR4A3 as the most significant differentially expressed genes (Figure S2). However, western blot analysis shows no substantial change in Grem1 between siCTL and siBMI-1 treated cells in Rh30, or in siBMI-1 treatments compared to control in Rh28 (Figure 12B). There is no substantial change in either Rh28 or Rh30 between the two treatments for NR4A3, and, moreover, not much baseline expression of this protein in these two cell lines either (Figure 12C).

C. Determining effects of BMI-1 on overall cell cycle and vitality

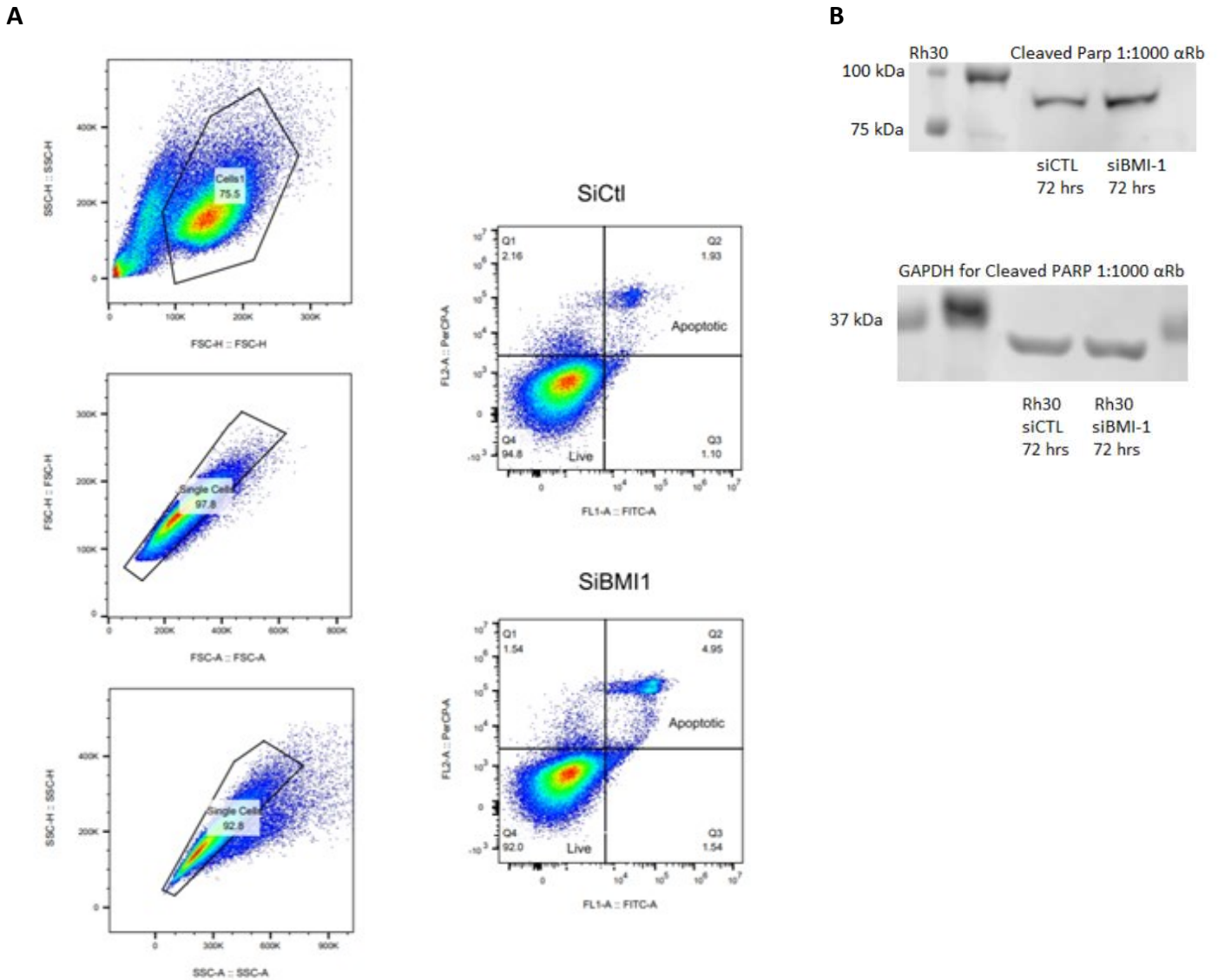


Figure 13. BMI-1 inhibition effects on apoptosis measured with A: Flow cytometry gating strategy for Annexin V/PI Staining for siBMI-1 vs. siCTL Rh30 cells; B: Cleaved PARP western blot analysis with siBMI-1 vs. siCTL Rh30 cells

Annexin V/PI staining for apoptosis shows a 3.02% increase in apoptotic cells within siBMI-1 treated Rh30 cells compared to control (Figure 13A). Figure S3 shows the failed BMI-1

knockdown validation for the Annexin V/PI staining. However, cleaved PARP, a marker for apoptosis, shows a more substantial increase in expression in validated siBMI-1 Rh30 lysates versus siCTL (Figure 13B).

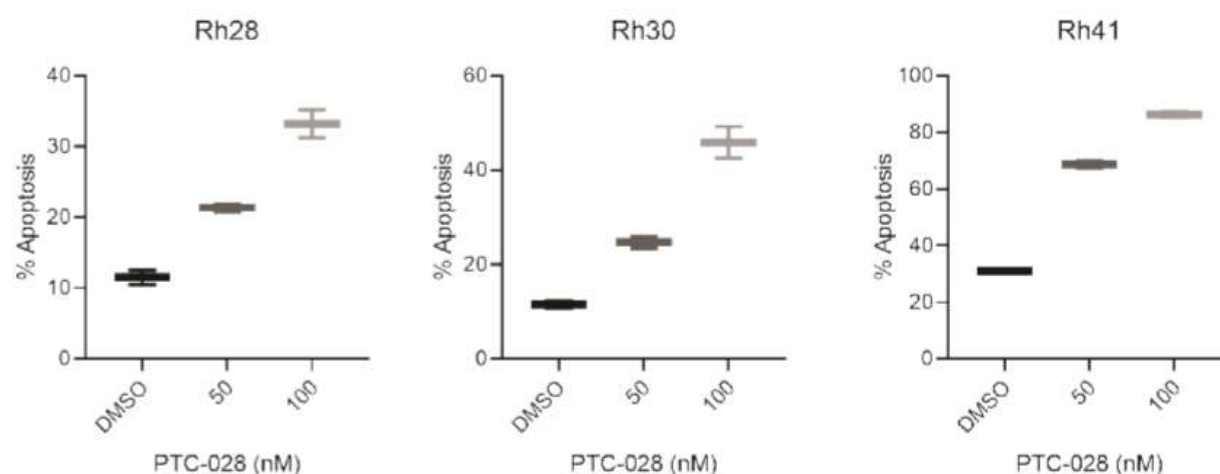


Figure 14. BMI-1 inhibition by PTC-028 effects on apoptosis of Rh28, Rh30, and Rh41 cell line *

Annexin V/PI staining of PTC-028 treated ARMS cell lines Rh28, Rh30, and Rh41, the gating strategy of which is modeled in/shown in Figure S4A, shows greater apoptosis with increasing drug. Treatment with PTC-028 at 100 nM shows a ~22% increase in apoptosis compared to DMSO control in Rh28, a ~32% increase in Rh30, and a ~53% increase in Rh41 (Figure 14). Cleaved PARP also increases with increasing drug treatment in Rh30 cells (Figure S4B).

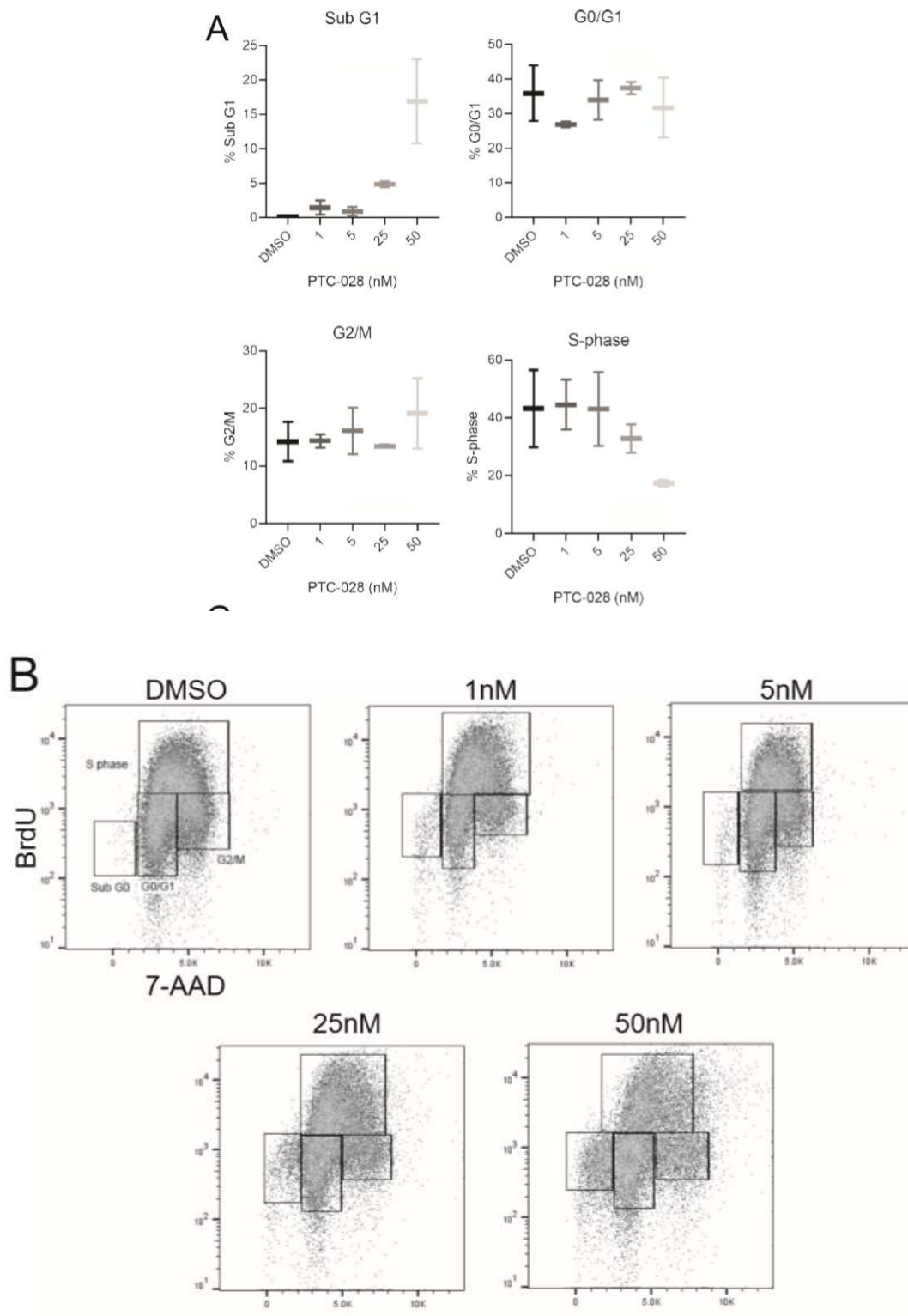


Figure 15. Cell cycle effects of BMI-1 inhibition by PTC-028 in Rh30 cells shown by BrdU/7-AAD staining (A) and the gating strategy for BrdU/7-AAD staining (B) *

BMI-1 inhibition by PTC-028 in Rh30 shows considerable changes in different cell cycle stages compared to DMSO treated Rh30. While increasing drug causes a relatively stable trend in the G0/G1 population of cells and an increasing trend in the G2/M population, it markedly increases the Sub-G1 population of Rh30 while diminishing the S phase population (Figure 15). There is a ~17% increase in the Sub-G1 population at 50 nM of PTC-028 per 10 cm plate compared to 0% of cells in the DMSO treatment. Furthermore, there is a 24% decrease in the S-phase population at 50 nM PTC-028 compared to DMSO control.

IV. Discussion

The purpose of this project was to clearly elucidate how BMI-1 affects the core proteins of the Hippo pathway and its downstream effectors in ARMS, as well as to study the impact of BMI1 on the cell cycle and apoptosis. whether BMI-1 has apoptotic and cell cycle effects.

A. *siRNA Transfection Validation*

The first step was to establish a siBMI-1 knockdown cell line in Rh28 and Rh30. siRNA used were chemically synthesized double-stranded small interfering RNA that target and degrade complimentary mRNA. Temporal knockdown optimization can vary per siRNA. siBMI-1, siRNA targeting BMI-1 transcripts, shows greater efficacy at 72 hours than 6 days because of these transient effects (Figure 8A-C). In other studies, observed kinetics of siRNA mediated RNAi peaked around 24 hours post-delivery and diminished within 48 hours (Rao et. al., 2009). The DharmaFECT transfection reagent has slight cellular toxicity that increases cell death over time, which accounts for the differential protein expression in the untreated, 72-hour siCTL, and 6-day siCTL Rh30 cells (Figure 8A-C).

Thus, with siBMI-1 transfection optimized at 72 hours of treatment, both BMI-1 protein and mRNA expression show substantial knockdown in Rh30 (Figure 8). Unfortunately, standardization of Rh28 72 hour-transfected siCTL and siBMI-1 samples for western blot analysis could not be completed due to the COVID-19 pandemic. Hence, only BMI-1 mRNA shows substantial knockdown in Rh28 at 72 hours of treatment (Figure 9).

B. BMI-1 Inhibition Turns on the Hippo Pathway

The Hippo western blot screen was given a generally qualitative analysis. Below is an analysis of BMI-1 inhibited by siRNA vs siCTL treatments in Rh30 for 72 hours. There is a slight decrease in Merlin expression compared to control (Figure 10A and S1). Whether this is an insignificant change or due to indirect upstream effects of BMI-1 is to be determined. There seems to be insignificant differential MST1 and LATS1 expression between treatment and control, as expected (Figure 10B and 10D). However, while phosphorylation does increase considerably for LATS1 with siRNA-mediated BMI-1 inhibition, it does not change compared to control for MST1 and may even decrease slightly (Figure 10C and 10E). This data could suggest that the Hippo pathway is turned on at LATS1 in Rh30, skipping MST1 phosphorylation-induced signaling, perhaps including Merlin signaling pathways.

YAP and p-YAP expression both decrease in Rh30 BMI-1 inhibition vs control, which is to be expected if p-YAP was being ubiquitinated and degraded in the proteasome, depleting cellular YAP (Figure 10G and 10H). There is some evidence to suggest that YAP is stabilized by physical interaction with BMI-1 in Ewing's Sarcoma (Hsu and Lawlor, 2010). Thus, this mechanistic proposal indicates that BMI-1 inhibition may sensitize YAP to degradation, signaling the initiation of the Hippo cascade. YAP depletion does not seem to affect TEAD transcription levels, as there is no or negligible change between siBMI-1 vs siCTL treatments in TEAD expression (Figure 10I and 10J). TEAD is a transcription factor family that has many non-Hippo cofactors, hence it is reasonable that TEAD expression is not directly impacted by YAP degradation or BMI-1 inhibition.

However, simply phosphorylating LATS1 and observing a degradation of YAP is not sufficient evidence to suggest that the Hippo pathway is turned on by BMI-1 inhibition. Downstream effectors of YAP-mediated oncogenic signaling must also show differential expression. Axl receptor tyrosine kinase is considered to be one critical downstream effector of YAP-dependent tumorigenesis, since knockdown of Axl shows decreased ability of YAP-overexpressing hepatocytes (MIHA) to proliferate and invade (Xu et. al., 2011). Knockdown of BMI-1 by siRNA seems to confer a small decrease in Axl expression (Figure 10K) compared to control. Whether this differential expression is significant is also to be determined.

NanoString, a multi-gene expression assay, was employed to recognize more potential downstream effectors of YAP/TAZ. At the mRNA level, NanoString identified Grem1 and NR4A3 as the most significant differentially expressed genes in PTC-028-mediated BMI-1 inhibition of Rh28 and Rh30 cells. Grem1 is a bone morphogenetic protein antagonist that shows positive correlation with TAZ expression levels in interstitial lung disease (ILD) (Noguchi et. al., 2017). NR4A3 is a transcriptional activator associated with chondrosarcoma and epithelial-myoeithelial carcinoma which is proposed to be modulated by YAP/TAZ in Ewing's Sarcoma (Rodríguez-Núñez, et. al., 2019). Validation at the protein level, however, indicates that BMI-1 inhibition by siRNA shows negligible differential expression of NR4A3 and Grem1 compared to control in both Rh28 and Rh30 (Figure 12B and 12C). Moreover, NR4A3 shows very little protein expression at baseline. Perhaps, though mRNA expression decreases, the NR4A3 and Grem1 are at steady-state protein levels when BMI-inhibition is induced. Another possible explanation is that PTC-028 is more effective at inhibiting BMI-1, enough to affect downstream effectors.

Interestingly, LATS2 shows a major decrease in expression in BMI-1 inhibition by siRNA compared to expression in siCTL in Rh30 (Figure 10F). LATS1 and LATS2 have evolved before the YAP-Hippo axis, and function in multiple other pathways. They often have similar functional purposes, but also have functions independent of each other. LATS1/2 both are downstream of cell cycle signaling, but LATS1 only is related to estrogen signaling and LATS2 is related to metabolism and p53 signaling (Furth and Aylon, 2017). While considered mostly tumor suppressive in function, LATS1/2 also seem to promote oncogenesis in some cancers, such as nasopharyngeal carcinomas and glioblastoma (Furth and Aylon, 2017). Hence, LATS1/2 have complex roles in cancer outside of the Hippo pathway, and one of those roles could explain the decrease in LATS2 when LATS1 seems to be activating the Hippo pathway.

However, the more compelling argument for the LATS2 expression decrease is that YAP/TAZ co-activation of TEAD directly activates LATS2, but not LATS1, gene expression. It has been proposed that this negative feedback loop between YAP/TAZ and its negative regulator, LATS2, serves to resist overexpression of YAP and increase Hippo cascade efficacy (Moroishi et al., 2015). Hence, if BMI-1 inhibition causes YAP to degrade, LATS2 is no longer necessary to downregulate high YAP levels and its expression cannot be signaled. This would provide evidence that the Hippo pathway is indeed being turned on with BMI-1 inhibition in Rh30, for YAP is being degraded and transactivation of downstream protein expression is being turned off.

BMI-1 inhibition by PTC-028 shows similar trends in Hippo pathway effects to BMI-1 inhibition by siRNA in Rh30. Furthermore, PTC-028 inhibition of BMI-1 seems to have stronger effects on Hippo proteins than siBMI-1. It is unlikely that the drug at IC50 causes overall protein

degradation/downregulation due to toxicity, because MST1 and TAZ protein levels change negligibly with increasing drug (Figure 11B and 11G). TAZ not being affected by BMI-1 inhibition further evidences that BMI-1 activates/stabilizes YAP to regulate the Hippo cascade. As drug is increased, there is more striking decrease in YAP (Figure 11F) and a slight decrease in TEAD1 expression unobserved in siBMI-1 treated Rh30 cells (Figure 11H). Intriguingly, MST1 phosphorylation and LATS1 protein levels appear to fluctuate with increasing PTC-028 in Rh30 (Figure 11C and 11D). Despite these fluctuations, the Hippo pathway also seems to be activated at LATS1/2 phosphorylation in the drug-mediated BMI-1 inhibition of Rh30.

On the other hand, there is a definite increase in MST1 phosphorylation at IC50 of drug in Rh28 (Figure 11B). Because LATS1/2 has an increase in phosphorylation at IC50, and both YAP and TEAD1 decrease in expression, this observation may suggest that the Hippo pathway is activated at MST1 phosphorylation in Rh28 once BMI-1 is inhibited below a threshold by PTC-028.

C. BMI-1 inhibition increases cellular apoptosis and diminishes progression to S-phase

An early apoptosis event is the flipping of inner surface phosphatidylserine to the outer surface. Annexin V binds specifically to phosphatidylserine on the outer surface, detecting all cells that have progressed to this apoptotic event. Because propidium iodide (PI) staining detects cell viability, employing the Annexin V/PI dual stain will detect cellular apoptosis in flow cytometry. Comparing siCTL and siBMI-1 treated Rh30 cells, BMI-1 inhibition only provides a slight increase in the apoptotic population in the Annexin V/PI staining (Figure 13A).

The cleavage of PARP is another apoptotic event. Blotting for cleaved PARP in a western blot shows a salient increase in apoptosis in the siBMI-1 treatment compared to control in Rh30 (Figure 13B). This discrepancy between western blot and flow cytometry data could be due to failed RNAi in the staining samples. However, because protein lysates utilized for Annexin V/PI staining could not be standardized, this conclusion cannot be reached (Figure S3). Therefore, the western blot data for cleaved PARP, in which the protein samples have been standardized and validated for BMI-1 inhibition by siRNA, appear more credible.

Fortunately, BMI-1 inhibition by PTC-028 shows a substantial and overall increase in apoptosis with increasing drug in Rh28, Rh30, and Rh41 (Figure 7). This observation indicates that the PTC-028 targeted therapy has strong therapeutic potential. Further evidencing PTC-028 and BMI-1 inhibition's anti-cancer effects is the BrdU/7-AAD staining assay.

Bromodeoxyuridine (BrdU) is a thymidine analog that incorporates into newly synthesized DNA, effectively identifying all proliferating cells defined by their progression through S phase. 7-aminoactinomycin D (7-AAD) is a dye that binds total DNA and, when used in conjunction with BrdU, can characterize cells in the G0/G1 and G2/M phases of the cell cycle based on 7-AAD staining intensities.

In PTC-028-mediated BMI-1 inhibition of Rh30 cells, increasing drug shows a considerable increase in dying/apoptotic cells and diminishing progression to S-phase. These effects become more pronounced at 25 and 50 nM of PTC-028 per 10 cm plate of cells (Figure 15A). The slight increase in the G2/M population with increasing drug may indicate cancer cells are being arrested at the G2/M checkpoint. This notion is further evidenced by the staggering decrease in S-phase progression as drug increases. Mechanistically, BMI-1 prevents cellular

senescence by transcriptional repression of the *Cdkn2a* locus, at which apoptosis-promoting checkpoint proteins p16^{INK4a} and p14^{ARF} are encoded (Douglas et. al., 2009). This data implies that BMI-1 inhibition by PTC-028 sensitizes Rh30 cancer cells to S phase apoptotic and cell arrest processes by upregulating checkpoint proteins.

V. Further Studies and Conclusions

Unfortunately, due to the Covid-19 pandemic, further validating studies could not be completed. Therefore, the focus of ongoing research should be first and foremost to test siBMI-1 effects on Rh28 and Rh41 at the protein level, determining BMI-1 mechanistic differences in various alveolar rhabdomyosarcoma lines. Moreover, replicates of the studies presented in this paper can help determine the significance of some unclear data. An important validating study would be to inhibit the proteasome and determine whether p-YAP expression increases, indicating whether YAP is truly being degraded by the initiation of the Hippo cascade. More downstream targets of YAP with tumorigenic effects should be identified and analyzed in the BMI-1 inhibition context. Furthermore, cell cycle and apoptotic effects of siRNA inhibition of BMI-1 should be better clarified in ARMS cell lines with more replicates of Annexin V/PI and BrdU/7-AAD staining analyses.

An interesting future study could be to determine if BMI-1 has any direct or physical interaction with the Hippo pathway in ARMS cell lines. This would help validate the mechanistic proposal that BMI-1 stabilizes YAP through physical interaction.

Our study has provided evidence that both BMI-1 inhibition by siRNA and PTC-028 turn on the Hippo contact inhibition pathway in Rh30 alveolar rhabdomyosarcoma cells, rescuing the pathway at LATS1 phosphorylation. Moreover, PTC-028 mediated BMI-1 inhibition turns on the Hippo pathway in ARMS Rh28 cells, perhaps at MST1 at the IC50 of the drug. Hence, BMI-1 overexpression in ARMS inhibits the Hippo pathway, allowing increasing tumorigenesis. BMI-1 inhibition by drug or siRNA also shows an increase in cellular apoptosis and drug treatment has

exhibited a decrease in cancer cell proliferation by hindering progression to S-phase. This data further clarifies BMI-1 mechanistic effects on alveolar rhabdomyosarcoma and presents BMI-1 inhibition by PTC-028 as a pioneering and powerful targeted therapy to treat this challenging and debilitating cancer.

VI. Bibliography

- Barr, FG. "Soft tissue tumors: Alveolar rhabdomyosarcoma." *Atlas of Genetics and Cytogenetics in Oncology and Haematology* 13(12) (January 2009): 981-985
- Chittock, EC, S Latwiel, TCR Miller, CW Müller. "Molecular architecture of polycomb repressive complexes." *Biochemical Society Transactions* 45(1) (February 2017): 193-205
- Dey, A, X Xiong, A Crim, SKD Dwivedi, SB Mustafi, P Mukherjee, L Cao, N Sydorenko, R Baiazitov, YC Moon, M Dumble, T Davis, and R. Battacharya. "Evaluating the Mechanism and Therapeutic Potential of PTC-028, a Novel Inhibitor of BMI-1 Function in Ovarian Cancer." *Molecular Cancer Therapeutics* 17(1) (January 2018): 39-49
- Douglas, D, JH Hsu, L Hung, A Cooper, D Abdueva, J van Doorninck, G. Peng, H Shimada, TJ Triche, and ER Lawlor. "BMI-1 promotes Ewing sarcoma tumorigenicity independent of *CDKN2A*-repression." *Cancer Research* 68(16) (August 2008): 6507-6515
- Furth, N, and Y Aylon. "The LATS1/LATS2 and LATS2/LATS1 tumor suppressors: beyond the Hippo pathway." *Nature Cell Death & Differentiation* 24 (June 2017): 1488-1501
- H Richly, L. Aloia, and L. Di Croce. "Roles of the Polycomb group proteins in stem cells and cancer." *Cell Death and Disease* 2 (September 2011): e204
- Halder G and RL Johnson. "Hippo signaling: growth control and beyond." *Development* 138(1) (January 2011): 9-22
- Hanahan, D. and RA Weinberg. "Hallmarks of Cancer: The Next Generation." *Cell* 144(5) (March 2011): 646-674
- Hsu, J.H. and E.R. Lawlor. "BMI-1 suppresses contact inhibition and stabilizes YAP in Ewing sarcoma." *Oncogene* 30(17) (2010) 2077-2085.
- Huang, R., N.K. Cheung, J. Vider, I.Y. Cheung, W.L. Gerald, S.K. Tickoo, E.C. Holland, and R.G. Blasberg. "MYCN and MYC regulate tumor proliferation and tumorigenesis directly through BMI1 in human neuroblastomas." *Faseb Journal* 25(12) (2011): 4138-4149
- Justice, RW, O Zilian, DF Woods, M Noll, and PJ Bryant. "The Drosophila tumor suppressor gene warts encodes a homolog of human myotonic dystrophy kinase and is required for the control of cell shape and proliferation" *Genes Dev* 9(5) (March 1995): 534-46

- Lawlor, ER and CJ Thiele. "Epigenetic changes in pediatric solid tumors: promising new targets." *Clinical Cancer Research* 18(10) (May 2012): 2768-2779
- Lim, SM, CJ Yoo, JW Han, YJ Cho, SH Kim, JB Ahn, SY Rha, SJ Shin, HC Chung, WI Yang, KH Shin, JK Rho, and HS Kim. "Incidence and Survival of Pediatric Soft Tissue Sarcomas: Comparison between Adults and Children." *Cancer Research and Treatment* 47(1) (August 2015): 9-17.
- Moroishi, T, HW Park, B Qin, Q Chen, Z Meng, SW Plouffe, K Taniguchi, F Yu, M Karin, D Pan, and K Guan. "A YAP/TAZ-induced feedback mechanism regulates Hippo pathway homeostasis." *Genes and Development* 29(12) (June 2015): 1271-1284
- Noguchi, S, A Saito, Y Mikami, H Urushiyama, M Horie, H Matsuzaki, H Takeshima, K Makita, N Miyashita, A Mitani, T Jo, Y Yamauchi, Y Terasaki, and T Nagase. "TAZ contributes to pulmonary fibrosis by activating profibrotic functions of lung fibroblasts." *Nature Scientific Reports* 7 (February 2017): 42595
- Parrish, JZ, K Emoto, LY Jan, and YN Jan. "Polycomb genes interact with the tumor suppressor genes hippo and warts in the maintenance of *Drosophila* sensory neuron dendrites." *Genes and Development* 21(8) (April 2007): 956-972
- Rao, DD, JS Vorhies, N Senzer, and J Nemunaitis. "siRNA vs. shRNA: Similarities and differences." *Advanced Drug Delivery Reviews* 61(9) (July 2009): 746-759
- Rodríguez-Núñez, P, L Romero-Pérez, AT Amaralab, P Puerto-Camacho, C Jordán, D Marcilla, TGP Grunewald, E de Alavaab, and J Díaz-Martín. "Hippo pathway effectors YAP/TAZ induce a EWS-FLI1-opposing gene signature and associate with disease progression in Ewing Sarcoma." *Journal of Pathology* 250(4) (December 2019)
- Schwartz, Y.B. and V. Pirrotta. "Polycomb complexes and epigenetic states." *Current Opinion in Cell Biology* 20(3) (April 2008): 266-273
- Scoles, DR, WH Yong, Y Qin, K Wawrowsky, and SM Pulst. "Schwannomin inhibits tumorigenesis through direct interaction with the eukaryotic initiation factor subunit c (eIF3c)." *Human Molecular Genetics* 15(7) (2006): 1059-1070
- St. John, MA, W Tao, X Fei, R Fukumoto, ML Carcangju, DG Brownsterin, AF Parlow, K McGrath, and T XU. "Mice deficient of Lats1/LATS1 develop soft-tissue sarcomas, ovarian tumours and pituitary dysfunction" *Nat. Genet.* 21(2) (February 1999):182-6.
- Staley, BK and KD Irvine. "Hippo signaling in *Drosophila*: recent advances and insights." *Developmental Dynamics* 241(1) (January 2012): 3-15

Wang, W, JJ Qin, S Voruganti, S Nag, J Zhou, and R Zhang. "Polycomb Group (PcG) Proteins and Human Cancers: Multifaceted Functions and Therapeutic Implications" *Medicinal Research Reviews* 35(6) (November 2015): 1220-1267

Xu, MZ, SW Chan, AM Liu, KF Wong, ST Fan, J Chen, RT Poon, L Zender, SW Lowe, W Hong, and JM Luk. "AXL receptor tyrosine kinase is a mediator of YAP-dependent oncogenic function in hepatocellular carcinoma." *Oncogene* 30(10) (March 2011): 1229-1240

VII. Non-Print References

1. American Cancer Society. "Survival Rates for Rhabdomyosarcoma by Risk Group." Atlanta: American Cancer Society; (July 2018); https://www.cancer.org/cancer/rhabdomyosarcoma/detection-diagnosis-staging/staging-survival-rates.html#written_by
2. American Cancer Society. Cancer Facts & Figures 2019. Atlanta: American Cancer Society; (2019); <https://www.ncbi.nlm.nih.gov/pmc/articles/PMC4296854/>
3. Selleckchem. "PTC-028" Catalog No. S8662: <https://www.selleckchem.com/products/ptc-028.html>
4. U.S. Cancer Statistics Working Group. U.S. Cancer Statistics Data Visualizations Tool, based on November 2018 submission data (1999-2016): U.S. Department of Health and Human Services, Centers for Disease Control and Prevention and National Cancer Institute (2019); <https://www.cdc.gov/cancer/dataviz>

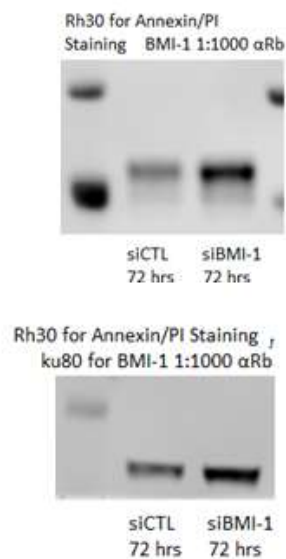
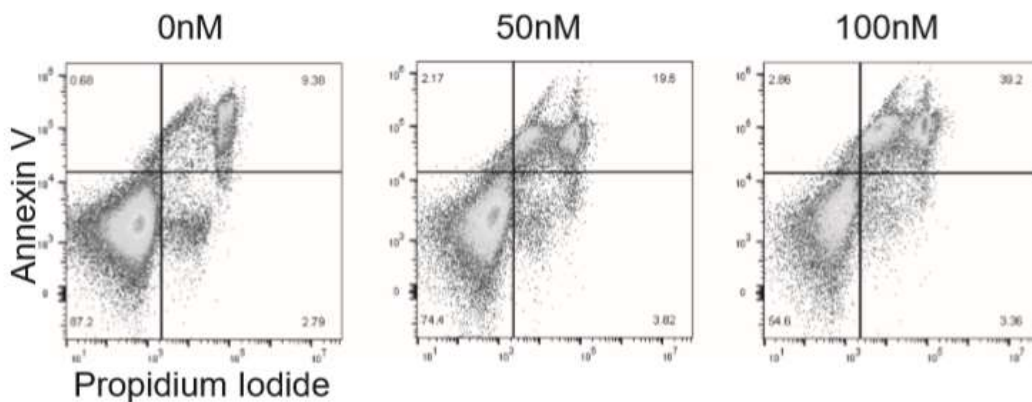


Figure S3. Failed siBMI-1 knockdown validation in Rh30 siRNA treated cells

A



B

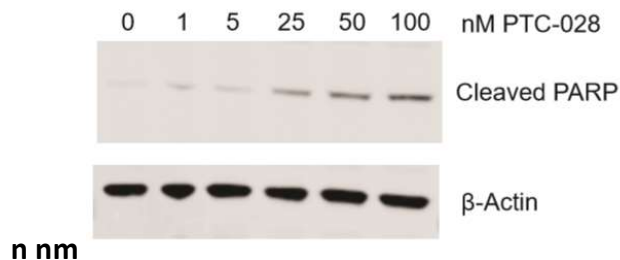


Figure S4. BMI-1 inhibition by PTC-028 effects on apoptosis shown by (A) Gating and treatment strategy for PTC-028 treated ARMS cell lines in Annexin V/PI staining, with Rh30 cells serving as a template; and, BMI-1 inhibition by PTC-028 effects on cleaved PARP (B)*